Journal of the Physical Society of Japan
Vol. 69, No. 7, July, 2000, pp. 2182-2187

Effect of Interface Roughness on GMR in Fe/Cr Multilayers

Ajay Gupta*, Amitesh Paul**, S. M. Chaudhari
and D. M. Phase

*Inter-University Consortium for DAE Facilities, University Campus,
Khandwa Road, Indore-452017, India*

(Received November 29, 1999)

Effect of interfacial roughness on Giant Magnetoresistance (GMR) in Fe/Cr multilayers has been studied by simultaneously depositing multilayers on a set of float glass substrates prepared with varying rms surface roughness. Morphological and other microstructural features of different multilayers are similar except for the interfacial roughness, thus allowing one to separate out the effect of interface roughness. GMR measurements on these multilayers show that increasing interfacial roughness causes GMR to decrease nonlinearly. GMR tends to saturate to a constant value for higher interfacial roughnesses because of the fact that different multilayers differ mainly in the correlated part of interfacial roughness.

KEYWORDS: magnetic films and multilayers, giant magnetoresistance, interface structure and roughness

§1. Introduction

Giant magnetoresistance (GMR) in metallic multilayers[1] continues to be a topic of great current interest. Extensive studies are being done in order to elucidate the origin of the underlying processes, *e.g.*, interlayer coupling and spin dependent scattering. The qualitative features of the interlayer coupling like the oscillatory behavior,[2,3] coexistence of a long and a short period of oscillations[4] and dependence of the oscillation period on the crystallographic orientation of the spacer layer[4,5] have been satisfactorily explained in terms of the RKKY type of interaction,[6] or in terms of quantum interferences due to confinement in ultrathin layers.[7] The spin dependence of electron scattering is understood in terms of the spin dependent electron states and the spin dependence of the scattering potential.[8,9] However, one of the aspects of the GMR phenomenon which are still not understood properly is the role of the interface structure in determining the GMR. Numerous experimental as well as theoretical studies have been done with an aim to elucidate the effect of the interface quality on GMR. Early theoretical studies predicted an increase in GMR with increase in interface roughness,[10,11] while some other calculations showed the existence of an optimal interface roughness.[12] A finite interface roughness can either enhance or decrease the GMR effect depending upon whether the spin-asymmetry for the interface and for the bulk scattering is of the same kind or not.[9] The effect of interface roughness is also expected to depend upon whether the roughness is perfectly random or there exist a correlation in the x-y plane.[8] More recently, *ab initio* calculations by Kudrnovský *et al.*,[13] for interlayer coupling in the presence of i) uncorrelated interfacial roughness and ii) interfacial interdiffusion, predicted a decrease in interlayer coupling and hence in GMR in the presence of both the types of imperfections. Experimental results on the effect of interface roughness on GMR are also conflicting. Fullerton *et al.* studied GMR in a number of Fe/Cr multilayers prepared under different sputtering pressures and power.[3] A substantial increase in GMR was observed in multilayers prepared at higher sputtering pressure which also showed a higher interface roughness as determined from X-ray reflectivity (XRR) measurements. Similar results were also obtained in a number of other studies in Fe/Cr system.[14,15] On the contrary, in the studies by Takanashi *et al.*,[16] and N. M. Rensing *et al.*,[17] on sputtered Fe/Cr multilayers it was concluded that smoother interfaces are necessary in order to increase GMR. Beliën *et al.*,[18] and Schad *et al.*,[19] varied the substrate temperature during deposition in order to vary the quality of the interfaces in MBE grown polycrystalline Fe/Cr multilayers. Besides effecting the interface quality the substrate temperature also effected other characteristics like the saturation resistivity ρ_s at 4.2 K and the residual resistance ratio ρ_{300}/ρ_s. However, they found a clear correlation between GMR and the interface quality. It was suggested that although interface roughness strongly suppresses the GMR, moderate step density at the interfaces can enhance the GMR. D. M. Kelly *et al.*,[20] studied the GMR in sputtered Fe/Cr multilayers as a function of the changes in interfacial roughness created by irradiation with 500 keV Xe ions. They argued that since GMR varies considerably with Cr layer thickness, much more reliable information can be obtained if the effect of interfacial roughness is studied in a single sample when its structure is modified by ion irradiation. They concluded that increased interfacial roughness enhances the GMR. However it may be noted that they also found a significant increase in structural coherence length of grains normal to the film plane with increasing irradiation dose, which may also influence the GMR. Increase in interfacial roughness as a result of

* E-mail: agupta@iucindore.ernet.in
** E-mail: prasanna@iucindore.ernet.in

thermal annealing in multilayers also resulted in a decrease in GMR[21, 22] More recently, studies have been done to get some quantitative information about the interface roughness dependence of GMR. Schad *et al.*[23, 24] determined the rms interface roughness and the in-plane correlation length from the XRR measurements done using anomalous scattering on a number of Fe/Cr multilayers. Multilayers with different interface roughness were prepared either by varying the substrate temperature[23] or by post deposition annealing treatment.[24] Effect of variation in antiferromagnetic coupling fraction (AFF) with substrate temperature was corrected for by measuring the saturation and remanent magnetizations M_s and M_r and taking AFF $= 1 - M_r/M_s$. They concluded that the GMR decreases almost linearly with increasing interface roughness.[23] In a more careful study with epitaxial Fe/Cr(001) superlattices with negligible bulk scattering[24] they concluded that GMR effect increases with decreasing lateral correlation length and increasing vertical correlation length. On the other hand, Velez *et al.*[25] varied the interface roughness by varying the sputtering pressure. They also corrected for the variation in AFF in a manner similar to that of Schad *et al.*[23] In contradiction to the work of Schad *et al.*,[23] in their case the GMR corrected for the variation in AFF was found to increase with interface roughness. It may be pointed out here that, it is somewhat ambiguous to use the value of M_r to correct for AFF, since a variation in the internal stresses as a result of the variations in the deposition conditions may affect M_r via stress induced anisotropy. Further, effects of any biquadratic coupling[26] can not be taken into account in this manner.

In the above studies, variations in the interfacial roughness are obtained either by varying the deposition conditions (sputtering gas pressure, sputtering power, substrate temperature) or by post deposition treatments (ion irradiation, thermal annealing). It may be noted that these parameters, besides affecting the interface quality, are also expected to effect other film properties like grain size and morphology, grain texture, internal stresses and defect concentration in the bulk of the layers etc. For example, Parkin *et al.* found that the deposition temperature effects the structural coherence length of grains ξ along the film normal, as well as the grain texture.[27] The GMR was found to increase with ξ. Grain texture is also known to effect GMR in Fe/Cr multilayers significantly.[28, 29] Modak *et al.*[30] specifically studied the effect of grain size on GMR in Co/Cu multilayers. Variation of ξ was achieved by introducing a Cu underlayer. GMR was found to increase with increase in ξ. The sputtering pressure has been found to effect the internal stresses in the film as evidenced by a decrease in lattice spacing normal to the film plane with sputtering pressure.[25] Variation in the density of defects in the bulk of the layers as a result of variation in sputtering rate or due to thermal annealing is also expected to effect the GMR through variation in the spin dependent scattering from the impurities in the bulk.[31] The contradictory results obtained in the above studies[3, 14-25] for the effect of interface roughness on GMR may largely be attributed to the neglect of the effects of associated changes in the morphological and other microstructural features of the films on GMR. Therefore, in the present work we have studied GMR in a set of multilayers prepared by simultaneous electron beam evaporation in an UHV environment on a number of float glass substrates having different surface roughnesses. Characterization of the multilayers using X-ray reflectivity (XRR), x-ray diffraction (XRD), conversion electron Mössbauer spectroscopy (CEMS) and Atomic Force Microscopy (AFM) shows that except for the interface roughnesses, other microstructural features of the multilayer (ML) like grain size, coherence length, grain texture, intermixing at the interface, internal stresses etc. are identical, thus allowing one to selectively study the effect of interface structure on the GMR.

§2. Experimental

Float glass was used as substrate for depositing multilayers. Substrates with varying surface roughness were prepared by etching the float glass substrates in dilute HF for varying periods of time. Six substrares with etching times of 0 s, 15 s, 60 s, 300 s, 600 s and 1200 s, designated as specimens 1 to 6 respectively, were taken. XRR measurements showed that the rms surface roughness varied non-monotonically with etching time. For comparison a substrate of ordinary microscopic slide glass (SG) was also used which has a significantly higher surface roughness as compared to float glass. Multilayers were deposited on these substrates simultaneously in a UHV chamber using two e-beam guns (TELEMARK Model No. 528). The base pressure in the chamber was 8.0×10^{-10} mbar. A residual gas analyzer (LEDAMASS Model LM501) attached to the system gave the partial pressures of Oxygen and hydrocarbons below 10^{-10} mbar. Fe and Cr layers (starting material 99.95% and 99.99% purity respectively) were deposited at a rate of .01 nm/s. The source to substrate distance was kept at 60 cm, in order to ensure uniformity of layer thickness (within 0.5%) on different substrates. Thicknesses of individual layers were controlled during deposition using a standard quartz crystal oscillator. Multilayers consisted of the following deposition sequence: substrate/Cr(10.0)/[Fe(3.0)/Cr(1.2)]×20/Fe (5.0), where the numbers in brackets give the layer thickness in nm. Cr spacer layer thickness of 1.2 nm corresponds to the first peak in the antiferromagnetic coupling between Fe layers.[3]

XRR and AFM were used to characterize the substrate as well as the multilayers. XRD was used to determine the grain texture and size of the multilayers. CEMS was used to get information about the intermixing at the interface. For XRR a powder X-ray diffractometer model D5000 of Siemens with Cu Kα radiation was used. In order to limit divergence of the X-ray beam, a 50 μm slit was introduced in the path of incident X-rays and a knife edge was kept touching the surface of the specimen. The micron sized gap between the film surface and the knife edge acts as a narrow slit. The reflectivity pattern was measured in the 2θ range of 0.2° to 4.0°, where θ is the angle of incidence of X-rays on the sample. AFM measurements were done in contact mode using Digital

Instruments Nanoscope-II. CEMS measurements were done using a gas flow proportional counter and a 50 mCi ^{57}Co source in Rh matrix. Since the multilayers were prepared with natural iron, each CEMS spectrum took about 5 days of data accumulation. Magnetoresistance at room temperatures was measured using standard four-probe-technique with a constant current source and a nanovoltmeter in an external field upto 1 Tesla. The field was applied parallel to the plane of the film and perpendicular to the electrical current which was also in the same plane.

§3. Results

Figure 1 shows the XRR pattern of the float glass substrates subjected to different etching treatments. The continuous curves represent the theoretical fit to the data obtained using the dynamical diffraction theory of Parrat.[32] In order to obtain a good theoretical fit it was found necessary to incorporate a thin surface layer with somewhat higher electron density, *e.g.*, in the case of unetched float glass, this surface layer was 3.0 nm thick with electron density 10% higher than that of the bulk: It is known that during the preparation of float glass diffusion of Sn takes place at the glass surface in contact with the bath, which would cause the electron density of the top surface layer to increase. The surface roughness as obtained from the fitting of the reflectivity data is given in column 3 of Table I. One may note that the surface roughness exhibits a non-monotonous variation with etching time: after reaching a maximum value of 1.25 nm for etching time of 300 s, it again decreases with further etching. This reflects some sort of layer by layer removal of the surface during etching: when a fractional atomic layer is removed by etching the roughness will increase, however when a complete atomic layer is removed the roughness will come down. This behavior of roughness was confirmed by repeating the etching experiment several times. It was found that the maximum obtainable roughness increases with the concentration of HF.

Figure 2 shows the reflectivity pattern of the multilayers deposited on different substrates. The first Bragg peak due to multilayer periodicity is clearly visible. However beyond the first Bragg peak the reflectivity pattern becomes obscure due to strong diffuse scattering. Presence of the Cr seed layer, an electron density gradient in the substrate and a possible oxidation of the Fe capping layer made it difficult to obtain a good theoretical fit to the experimental data. However, the following information could be obtained: i) from the position of the Bragg peak one can find that the bilayer periodicity is 4.4 nm instead of the designed value of 4.2 nm. This difference may be due to some error in tooling factor of the thickness monitor. ii) height of the Bragg peak which is related to the average interface roughness, decreases with the increasing substrate roughness, confirming that the roughness of the substrate is at least partly transferred to the successive layers.

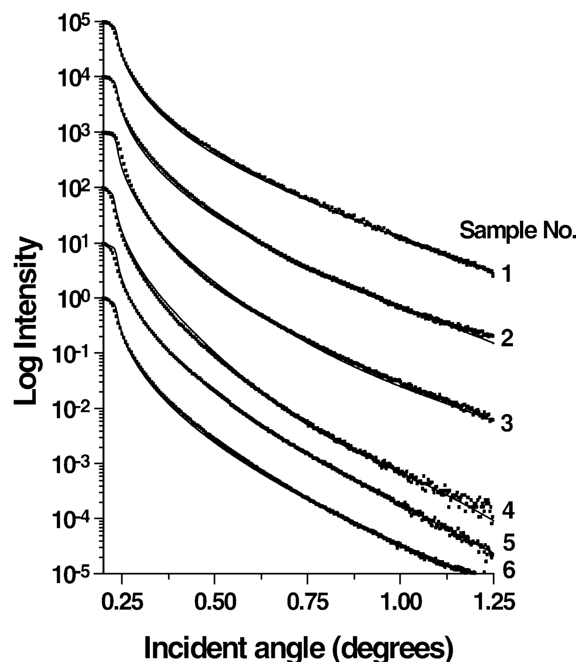

Fig. 1. X-ray reflectivity scans of float glass (FG) substrates with different etching times. The continuous curves represent the theoretical fits to the data. For clarity, various curves are shifted relative to each other along the y-axis.

Figure 3 gives a representative XRD pattern of specimen 1. XRD measurements showed that the films have a texture along (110) direction. However the texture does not vary from sample to sample. The width of (110) reflection was used to determine the structural coherence

Table I. Microstructural parameters of Fe/Cr multilayers on float glass (FG) substrates with different etching times and on microscopic slide glass (SG) as determined from XRR, XRD and AFM and CEMS measurements. σ is the rms roughness of the glass substrates after etching for different periods of time. The relative area under the broad hyperfine field component in the CEMS gives the fraction of total iron atoms located at the interfaces and is a measure of the thickness of the intermixed layer. The last coloumn gives the saturation magnetoresistance of the multilayer.

Sample No.	Time of etching (s)	RMS roughness σ (nm)	d-spacing of (110) planes (nm)	Structural coherence length ξ (nm)	Average grain size in x-y plane (nm)	Fraction of the total iron atoms at the interfaces (%)	GMR (%)
1	0	0.67 ± 0.05	$.2025 \pm 0.0005$	16.3 ± 1.0	248	26	3.52 ± 0.01
2	15	0.77	.2026	15.3	290	—	3.08
3	60	0.92	.2025	15.6	295	—	2.94
4	300	1.25	.2025	15.5	291	26	2.83
5	600	0.95	.2028	15.9	266	25	3.19
6	1200	0.85	.2029	16.1	261	—	3.22
SG	—	3.50	.2028	16.0	225	—	2.39

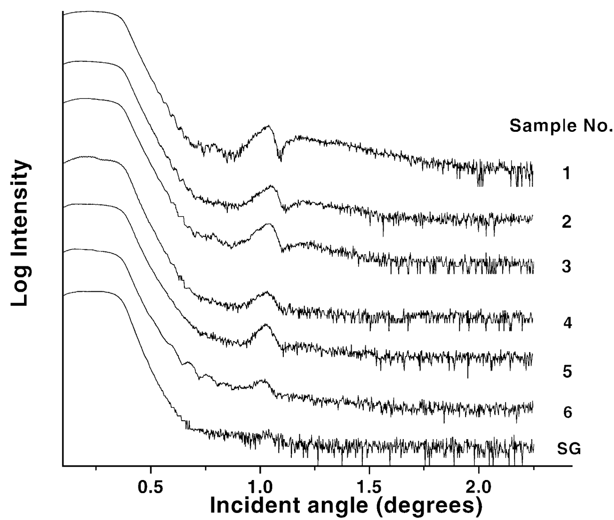

Fig. 2. X-ray reflectivity scans of Fe/Cr multilayers on float glass (FG) substrates with different etching times and on microscopic glass slide (SG). For clarity, various curves are shifted relative to each other along the y-axis.

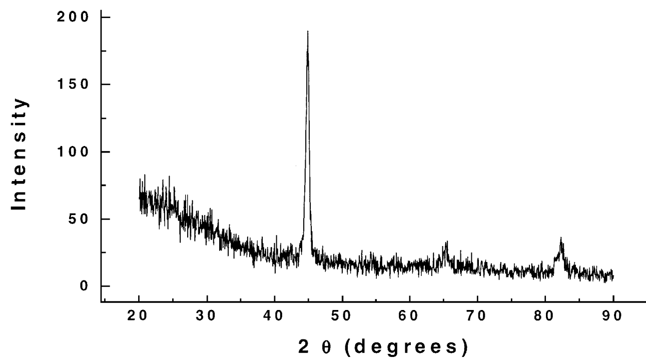

Fig. 3. X-ray diffractogram of the specimen 1 taken in an asymmetric Bragg-Brentano geometry with the angle of incidence kept fixed at 0.5°.

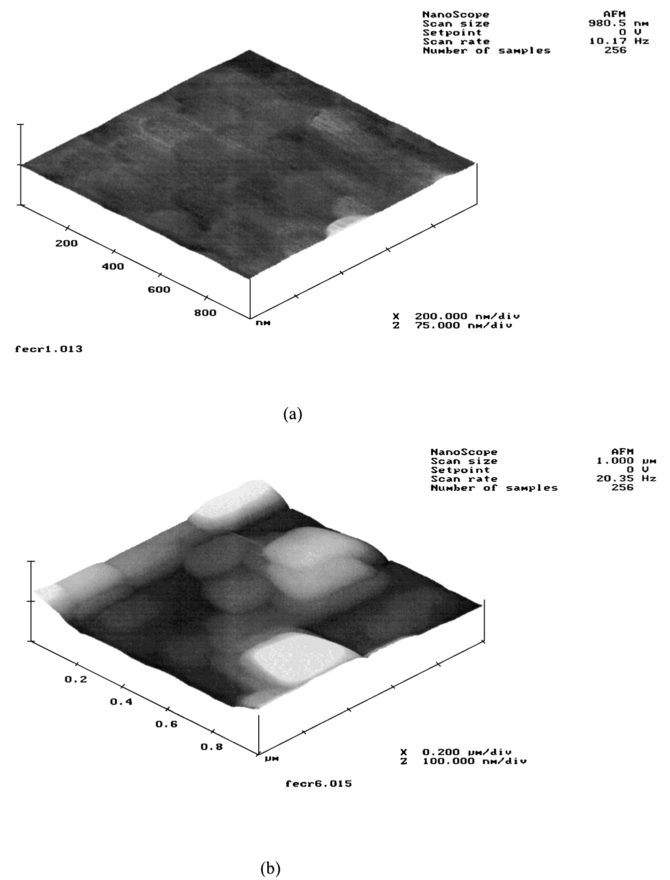

Fig. 4. AFM micrographs of two representative Fe/Cr multilayers on a) an unetched float glass substrate (sample 1) and (b) on a float glass etched for 600 seconds (sample 5).

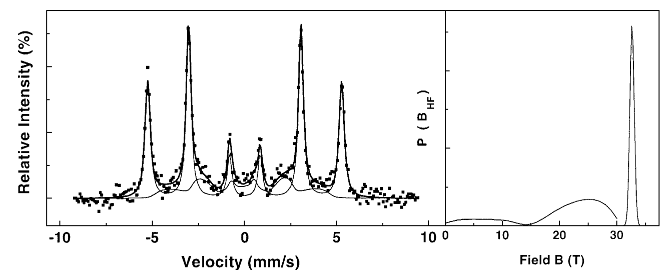

Fig. 5. Conversion electron Mössbauer spectrum of the specimen 1. The continuous curve represent theoretical fit to the spectrum with two hyperfine field distributions. The narrow distribution corresponds to the Fe atoms in the bulk of a layer, while the broad distribution corresponds to the iron atoms at the interface.

length ξ of grains along the momentum transfer vector q using the Scherrer method, and is reported in Table I. Since in the present case an asymmetric Bragg-Brentano geometry was used for XRD measurements, the momentum transfer vector for the (110) reflection made an angle ~22.5° from the film normal. From Table I it may be noted that ξ is several times the thickness of individual layers indicating a high degree of coherency between adjacent Fe and Cr layers. Further, one finds that ξ does not vary with substrate roughness. The d-spacing of (110) planes as calculated from the position of (110) reflection is also reported in Table I. The d-value and hence the internal stresses in the film also do not vary from sample to sample.

Figure 4 gives some representative AFM pictures of the multilayers. The polycrystalline nature of the films is clearly visible. For each sample ten different frames of $1\,\mu\text{m} \times 1\,\mu\text{m}$ were taken and the average grain size in the film plane was calculated. The results are reported in Table I. CEMS measurements were done in specimens 1, 4 and 6. Figure 5 gives a representative Mössbauer spectrum of specimen 1. All the Mössbauer spectra were fitted with two distributions of hyperfine magnetic fields and the results of fitting are also shown in Fig. 5. The distribution in the range $28\,\text{T} < B_{hf} < 36\,\text{T}$ corresponds to the bulk of the iron layers while the broad distribution in the range $0\,\text{T} < B_{hf} < 30\,\text{T}$ corresponds to the iron atoms at the interfaces. The fraction of total iron atoms located at the interfaces, which is proportional to the relative area under the broad sextet, is a measure of the thickness of the intermixed layer at the interface and is

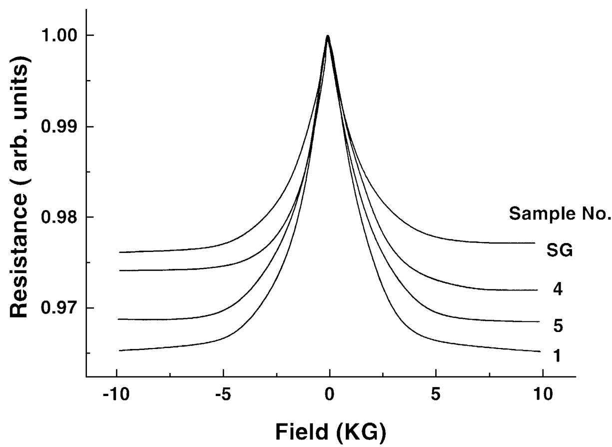

Fig. 6. Resistivity versus in-plane magnetic field curves at RT for some representative Fe/Cr multilayers *e.g.* on unetched float glass substrate (sample 1), on float glass etched for 300 seconds (sample 4), on float glass etched for 600 seconds (sample 5) and on microscopic glass slide (SG).

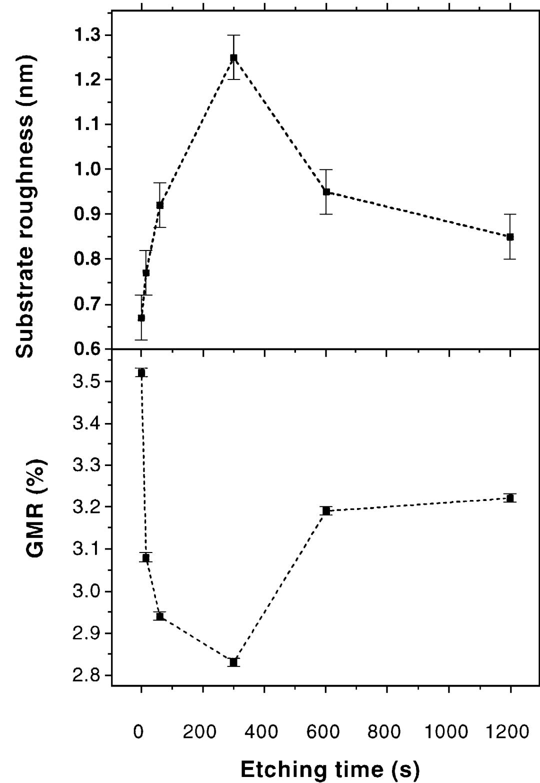

Fig. 7. Variation of a) surface roughness σ, and b) percentage GMR with the etching time.

reported in Table I. Fig. 6 gives the field dependence of the magnetoresistance of some of the samples. The giant magnetoresistance defined as $\frac{R_o - R_s}{R_s} \times 100$ with R_o and R_s being respectively the resistance values at zero and saturating fields, is also reported in Table I.

§4. Discussions

Perusal of Table I shows that grain size, grain texture, structural coherence length ξ, internal stresses and the thicknesses of the interface layers are similar for all the multilayers grown on different substrates. Furthermore, since all the films were deposited simultaneously, the deposition conditions like deposition rate and substrate temperature are identical for all the specimens. Therefore, the individual layer thicknesses as well as the density of defects in the bulk of the layers is expected to be similar. Thus, the only difference between various multilayers deposited on different substrates is in their interface roughness, and the observed variation in GMR can solely be attributed to variation in the interface roughness. In Fig. 7 are plotted the variations of the roughness and GMR as a function of the etching time. GMR decreases with increasing roughness. It is interesting to note that with increase in etching time, as the substrate roughness decreases for etching time beyond 300 s, the GMR of the corresponding multilayers also shows an increase. Thus, the variation in GMR is highly correlated with that in the roughness. From Fig. 8 one finds that, although the GMR decreases monotonically with increase in roughness, its dependence on the roughness is not linear. Initially the GMR decreases at a faster rate with increase in the roughness and for higher roughness tends to saturate to a constant value. This point is further supported by the observed value of GMR in the specimen prepared on microscopic slide glass: although in this specimen the roughness is so large that the multilayer Bragg peak is almost totally washed off, the decrease in GMR is not so large.

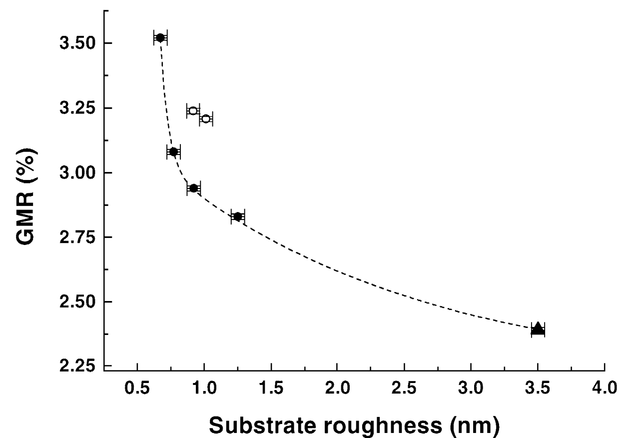

Fig. 8. The percentage GMR of Fe/Cr multilayers as a function of rms surface roughness of the substrates. The filled circles represent the data of specimens 1–4. The open circles represent the data of specimens 5 and 6 in which the growth morphology of the layers differs from that in specimens 1–4. Filled triangle represents the data point of the multilayer on slide glass.

From Fig. 8 it may be noted that the GMR of the multilayers prepared on the substrate etched for longer period of time is a little higher than that in the multilayers on substrates with similar roughness but etched for a shorter duration of time. This difference in GMR may be related to a difference in their growth morphology as seen from AFM pictures (Fig. 4). One finds that for specimen 5 and 6 the films show island type of growth, in contrast to the films 1–4 where the growth is more uniform. The cause of this difference in the growth morphology is not

clear, however, it should be related to the variation in the surface topology of the substrate with etching.

The difference in the interfacial roughness in different multilayers is essentially due to the difference in the roughness of their substrate which is transmitted to the successive layers. Thus, the difference among various multilayers is expected to be in their correlated part of the interfacial roughness. The uncorrelated roughness in all the multilayers is expected to be similar in magnitude because of the identical conditions of deposition. The saturation behavior in GMR with interface roughness is expected to be due to this correlated nature of the interfacial roughness. Otherwise, for a spacer layer thickness of 1.2 nm, an uncorrelated roughness of 3.5 nm (in the microscopic slide glass substrate) would have completely destroyed the multilayer structure and no GMR would have been observed in this multilayer.

§5. Conclusions

In conclusion, the effect of interface roughness on GMR in Fe/Cr multilayers has been determined by measuring GMR in a set of samples prepared in a controlled manner, so as to keep all the morphological and other characteristics similar except for the interface roughness. GMR decreases with interfacial roughness in a nonlinear manner and tends to saturate for higher values of roughnesses. This saturation behavior of GMR with roughness is expected to be due to the fact that different multilayers differ mainly in their correlated part of the interfacial roughness.

1) M. N. Baibich, J. M. Broto, A. Fert, F. Nguyen van dau, F. Petroff, P. Etienne, G. Creuzet, A. Friedrich and J. Chazelas: Phys. Rev. Lett. **61** (1988) 2472.
2) S. S. P. Parkin, N. More and K. P. Roche: Phys. Rev. Lett. **64** (1990) 2304.
3) E. E. Fullerton, M. J. Conover, J. E. Mattson, C. H. Sowers and S. D. Bader: Appl. Phys. Lett. **63** (1993) 1699; E. E. Fullerton, D. M. Kelly, J. Guimpel, I. K. Schuller and Y. Bruynserade: Phys. Rev. Lett. **68** (1992) 859.
4) M. T. Johnson, S. T. Purcell, N. W. E. Megee, R. Coehoorn, J. Aan de Stegge and W. Hoving: Phys. Rev. Lett. **68** (1992) 2688; D. H. Mosca, F. Petroff, A. Fert, P. A. Schroeder, W. P. Pratt Jr., R. Laloee and S. Lequien: J. Magn. Magn. Mater. **94** (1991) L1.
5) S. S. P. Parkin, R. Bhadra and K. P. Roche: Phys. Rev. Lett. **66** (1991) 2152.
6) Y. Yafet: Phys. Rev. B **36** (1987) 3948; P. Bruno, C. Chappert: Phys. Rev. Lett. **67** (1991) 1602.
7) P. Bruno: Phys. Rev. B **52** (1995) 411.
8) Hood R. Q., Falicov L. M. and Penn D. R.: Phys. Rev. B **49** (1994) 368.
9) J. Barnas and Y. Bruynserade: Phys. Rev. B **53** (1996) 5449.
10) R. E. Camley and J. Barnas: Phys. Rev. Lett. **63** (1989) 664.
11) Y. Asano, A. Oguria and S. Maekawa: Phys. Rev. B **48** (1993) 6192.
12) J. Barnas, A. Fuss, R. E. Camley, P. Grüberg and W. Zinn: Phys. Rev. B **42** (1990) 8110.
13) J. Kudrnovský, V. Drchal, I. Turek, M. Šob and P. Weinberger: Phys. Rev. B **53** (1996) 5152.
14) H. Nakashini, A. Okiji and H. Kasai: J. Magn. Magn. Matter. **126** (1993) 451.
15) F. Petroff, A. Barthelemy, A. Hamzic, A. Fert, P. Etienne, S. Lequien and G. Cruzet: J. Magn. Magn. Matter. **93** (1991) 95.
16) K. Takanashi, Y. Obi, Y. Mitani and H. Fujimori: J. Phys. Soc. Jpn. **61** (1992) 1169.
17) N. M. Rensing, A. P. Payne and B. M. Clemens: J. Magn. Magn. Mater. **121** (1993) 436.
18) P. Beliën, R. Schad, C. D. Potter, G. Verbanck, V. V. Moshchalkov and Y. Bruynserade: Phys. Rev. B **50** (1994) 9957.
19) R. Schad, J. Barnas, P. Beliën, G. Verbanck, C. D. Potter, H. Fisher, S. Lefebvre, M. Bessiere, V. V. Moshchalkov and Y. Bruynseraede: J. Magn. Magn. Mater. **156** (1996) 39.
20) David M. Kelly, Ivan Schuller, V. Koreniviski, K. V. Rao, Kim K. Larsen, J. Bottiger, E. M. Gyorgy and R. B. Van Dover: Phys. Rev. B **50** (1994) 3481.
21) E. M. Ho and A. K. Petford-Long: J. Magn. Magn. Mater. **156** (1996) 65.
22) L. H. Laider, B. J. Hickey, T. R. A. Hickey, T. R. A. Hase, B. K. Tanner, R. Schad and Y. Bruynserade: J. Magn. Magn. Mater. **156** (1996) 332.
23) R. Schad, P. Beliën, G. Verbanck, C. D. Potter, H. Fisher, S. Lefebvre, M. Bessiere, V. V. Moshchalkov and Y. Bruynseraede: Phys. Rev. B **57** (1998) 13692.
24) R. Schad, P. Beliën, G. Verbanck, V. V. Moshchalkov, Y. Bruynseraede, H. Fisher, S. Lefebvre and M. Bessiere: Phys. Rev. B **59** (1999) 1242.
25) M. Velez and Ivan Schuller: J. Magn. Magn. Mater. **184** (1998) 275.
26) J. C. Slonczewiski: Phys. Rev. Lett. **67** (1991) 3172; A. Schreyer, J. F. Ankner, Th. Zeidler, H. Zabel, M. Schäfer, J. A. Wolf, P. Grünberg and C. F. Majkrzak: Phys. Rev. B **52** (1995) 16066.
27) S. S. P. Parkin and B. R. York: Appl. Phys. Lett. **62** (1993) 1842.
28) Eric E. Fullerton, M. J. Conover, J. E. Mattson, C. H. Sowers and S. D. Bader: Phys. Rev. B **48** (1993) 15755.
29) José M. Colino, Ivan K. Schuller, R. Schad, C. D. Potter, P. Beliën, G. Verbanck, V. V. Moshchalokov and Y. Bruynserade: Phys. Rev. B **53** (1996) 766.
30) A. R. Modak, David J. Smith and S. S. P. Parkin: Phys. Rev. B **50** (1994) 4232.
31) E. Yu. Tsymbal and D. G. Pettifor: Phys. Rev. B **54** (1996) 15314.
32) L. G. Parratt: Phys. Rev. **95** (1954) 359.